Mechanically induced cyclic metastable phase transformations of Zr_2Ni alloys

M. Sherif El-Eskandarany*
Mining, Metallurgical and Petroleum Engineering Department, Faculty of Engineering, Al-Azhar University, Nasr City, 11371 Cairo, Egypt

A. Inoue
Institute for Materials Research, Tohoku University, Katahita 2-1-1 Sendai, Miyagi 980-8577, Japan
(Received 13 January 2007; published 14 June 2007)

Cyclic crystalline-glassy-crystalline phase transformations have been investigated during high-energy ball milling of tetragonal-Zr_2Ni alloy powders using mechanical disordering (MD) method. The results show that the metastable fcc-Zr_2Ni alloy powders which is obtained after 173 ks of MD time, transforms into a new metastable phase of nanocrystalline big cube-Zr_2Ni upon milling for 360 ks. The lattice parameters a_0 for the metastable-fcc and big-cube phases were calculated and found to be 0.451 nm and 1.226 nm, respectively. The obtained big-cube phase subsequently transforms to a single glassy phase after 540 ks of MD time. This obtained glassy phase, however, devitrificated into the same metastable big-cube phase upon increasing the MD time to 720 ks. As the MD time increases (806–900 ks), the obtained nanocrystalline big-cube phase transforms into the pervious metastable fcc-Zr_2Ni phase, indicating a cyclic-phase transformations between the three obtained metastable phases. Such cyclic phase transformations are observed several times during the milling procedure. On the basis of our results, the destabilizing effect of the defects created by the milling media (balls) is responsible for such mechanically induced solid-state devitrification that leads to the cyclic transformations.

DOI: 10.1103/PhysRevB.75.224109 PACS number(s): 61.43.Dq, 81.20.Wk, 05.70.Fh, 64.60.My

I. INTRODUCTION

Because of their exciting properties, metallic glasses[1,2] have attracted many metallurgists and materials scientists.[2–6] This class of materials has unique behaviors not found when the same alloys are in their stable crystalline states. They may possess unusual corrosion resistance, high hardness, unique mechanical ductility and yield strength, and high magnetic permeability with low coercive force. Hence, metallic glasses have been considered as promising candidates for several technical applications.[7,8] However, glassy alloys can be obtained by several ways of fabrications; ball-milling technique, using mechanical alloying[9] (MA) method, has been considered as a powerful tool[10] for fabrication of wide varieties of glassy powders (e.g., Refs. 11–17), including those systems that cannot be synthesized by the conventional melting and casting techniques.[18–20] Consolidation of these powders within their supercooled liquid regions leads to the formation of fully dense objects.[21–23]

Because Zr-Ni is the best known metal-metal glassy binary system, which can be made amorphous by several techniques over a wide range of composition, extensive studies have been made and reported on the crystallization and kinetics of this system. The present study has been undertaken to investigate the structural changes that take place upon room-temperature mechanical disordering[24] (MD) crystalline powders of tetragonal-Zr_2Ni, using high-energy ball mill. The stability of the obtained metastable powders (fcc-Zr_2Ni, big cube-Zr_2Ni, and glassy Zr_2Ni) against the shear and impact forces that are generated by the milling media and the subsequent devitrifications were demonstrated by subjecting the powders to longer MD times. Thus, the possibility of mechanically induced solid-state devitrifications (MISSD) could be investigated. For this purpose, x-ray diffraction, scanning and transmission electron microscopies, differential scanning calorimetry, and differential thermal analysis have been used to monitor the structural changes and the thermal stability of the mechanically disordered powders.

II. EXPERIMENTAL PROCEDURE

An ingot of $Zr_{67}Ni_{33}$, obtained by arc-melting a mixture of Zr (99.9 at. %) and Ni (99.9 at. %) metals, was crushed down into particles, using a tempered chrome steel mortar and pestle. The ground particles were then screened to obtain finer powders (50–60 μm in diameter) and used as the starting materials for MD process. The starting powders were charged into tempered chrome steel vials (250 ml in volume) and sealed together with 50 tempered chrome steel balls (10 mm in diameter) in an argon atmosphere glovebox. The ball-to-powder weight ratio was maintained at 14:1. The MD process was performed in a planetary ball mill (Fritsch P5) at a rotation speed of 2.1 s^{-1}. In order to avoid an increase in the vial temperature, the milling procedure was periodically interrupted every 1.8 ks and then halted for 1.8 ks under a continuous flow of air. The MD experiments were performed two or three times under the same experimental conditions to confirm the reproducibility of the results. The ball milling was stopped after selected milling times and a small amount (about 500 mg) of powders was taken from the vials in the glovebox. The as-milled samples were characterized by means of x-ray diffraction (XRD) employing Cu $K\alpha$ radiation, transmission electron microscopy (TEM), using a 300 kV field emission microscope, scanning electron microscopy (SEM) using 15 kV field emission electron microscope, and differential scanning calorimetry (DSC) at a constant heating rate of 0.67 K/s and under flow of a purified argon

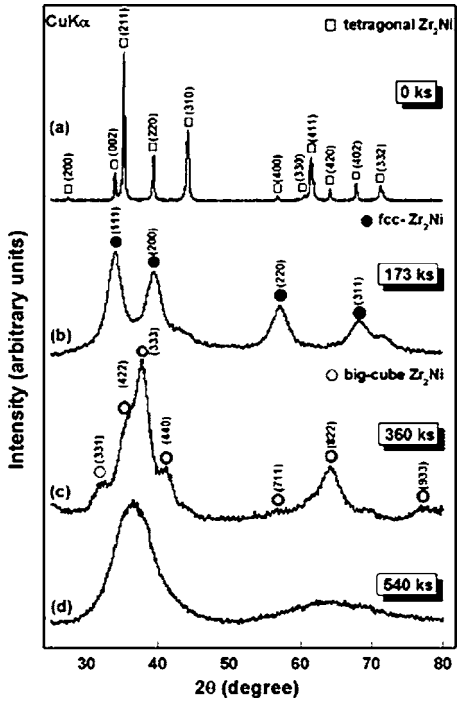

FIG. 1. XRD patterns of ball-milled Zr_2Ni powders after (a) 0 ks, (b) 173 ks, (c) 360 ks, and (d) 540 ks of MD time.

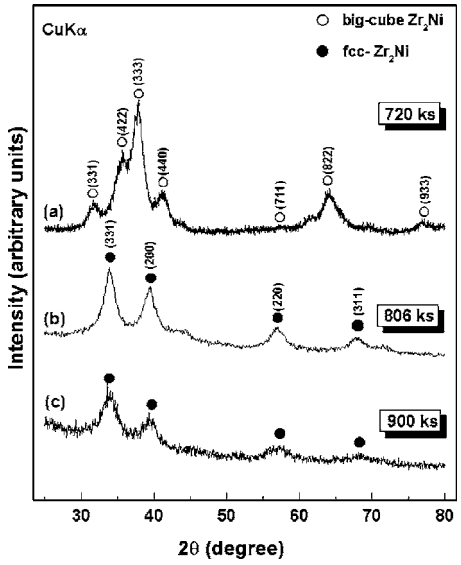

FIG. 2. XRD patterns of ball-milled Zr_2Ni powders after (a) 720 ks, (b) 806 ks, and (c) 900 ks of MD time.

gas. High-resolution transmission electron microscopy (HRTEM)/energy dispersive spectroscopy (EDS), using an electron beam of 5 nm has been employed for analyzing the concentration of Zr and Ni, and the degree of iron contamination in the milled powders. In addition, the oxygen content was determined by the helium carrier fusion-thermal conductivity method.

Annealing the powder samples was performed at the desired temperatures in sealed copper DSC cells under continuous flow (2.5 ml s^{-1}) of purified argon (99.999 wt. %) flow. As soon as the annealing procedure is achieved, the DSC was rapidly cooled and the samples were subsequently removed from the DSC heating chamber. The as-annealed samples were structurally analyzed by means of XRD and TEM and EDS techniques.

III. RESULTS

A. Structural changes with the MD time

1. XRD analysis

We will first begin with presenting the structural changes that took place in the starting materials of tetragonal Zr_2Ni alloy powders during the several stages of MD time. The XRD patterns of the ball-milled powders after selected MD times are displayed in Figs. 1 and 2. The sample at the starting stage of MD (0 ks) is a single phase of polycrystalline tetragonal-Zr_2Ni (□) and does not show the existence of any other phases, indicated by the presence of sharp indexed Bragg peaks of the starting ordered phase [Fig. 1(a)]. These Bragg peaks no longer appeared in the sample that was milled for 173 ks of MD and a new set of broad Bragg lines corresponding to fcc structure (●), which come from the reflections of (111), (200), (220), and (311) planes, appeared [Fig. 1(b)]. The analysis of the Bragg peaks for this new obtained phase confirmed the formation of a metastable fcc-Zr_2Ni (fcc-Zr_2Cu structure[11]) and its lattice parameter a_0 was calculated to be 0.451 nm.

This obtained fcc-Zr_2Ni metastable phase is not capable enough to withstand against the mechanical imperfections that came from the milling media and surprisingly transformed into a new crystalline phase (○) after 360 ks of MD time [Fig. 1(c)]. Careful analysis of the diffracted peaks in Fig. 1(c) suggests that the powders at this stage of MD reveal polycrystalline structure corresponding to Zr_2Ni structure [$E9_3$ structure, space group $Fd3m$ (Ref. 25)]. The lattice constant a_0 of this crystalline phase was calculated to be 1.226 nm, being in fair agreement with previously reported values for big-cube Zr_2Ni (1.2270 nm) (Ref. 23) and Zr_2Cu (1.2263 nm).[11] When the MD time is increased to 540 ks, all of the Bragg peaks corresponding to the formed big-cube phase have already disappeared and clear broad diffuse haloes appear, implying the formation of a single amorphous phase with no indication of precipitation of any residual crystalline phases [Fig. 1(d)].

The XRD pattern of the sample that was obtained after continuous ball milling for 720 ks of MD time is displayed in Fig. 2(a). Obviously, the amorphous phase is devitrificated into a nanocrystalline phase, characterized by the disappearance of the halo-diffraction peaks and the appearance of Bragg lines of a crystalline phase (○). Surprising came from when the analysis of the diffracted lines in Fig. 2(a) indicates that the yielded crystalline phase is a big-cube Zr_2Ni that has a_0 similar to that one, which was previously formed after 360 ks of MD time [Fig. 1(b)].

The stability of the yielded big-cube phase against the mechanical deformation during ball milling procedure has been realized so that the powders were further milled to 806 ks. As it is expected, this phase was transformed to a

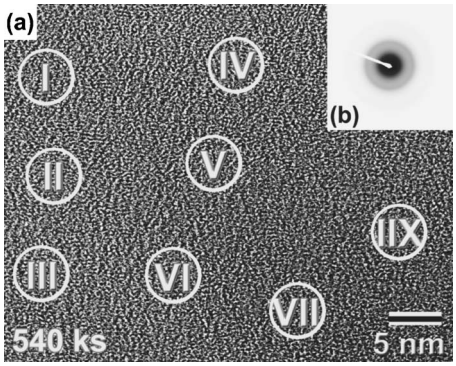

FIG. 3. (a) HRTEM image and (b) the corresponding SADP of ball-milled Zr_2Ni powders after 540 ks of MD time. The indexed circles in image (a) refer to the EDS examined regions and the analytical results are listed in Table I.

different metastable phase, indicated by the shown Bragg peaks in Fig. 2(b), which corresponds to an fcc-Zr_2Ni metastable phase. This fcc-metastable phase has almost the same a_0 of that phase, which obtained after milling for 173 ks [see Fig. 1(b)]. This would suggest cyclic-metastable-metastable-phase transformations.[26] Increasing the MD time to 900 ks does not lead to any further phase transformations and the end product still maintains its fcc structure, as displayed in the XRD pattern in Fig. 2(c). The obvious broadening in the Bragg lines of this metastable phase indicates the formation of a nanocrystalline phase.

2. TEM observations and local compositional analyses

The image of the HRTEM of the sample after 540 ks of MD time is shown in Fig. 3(a) together with the corresponding selected area diffraction pattern (SADP) [Fig. 3(b)]. Overall, the sample, which appears featureless and homogeneous in its internal structure, shows a maze contrast with no indication of precipitations of any crystalline phases [Fig. 3(a)], implying the homogeneity in structure within the nanoscale. Moreover, the SADP displays a typical halo diffraction (diffuse halo) of an amorphous phase [Fig. 3(b)]. The absence of any crystalline contrast [Fig. 3(a)] and the hardly vision of sharp rings or spots [Fig. 3(b)] would indicate the formation of fully amorphous phase. The EDS technique was employed to ensure the local composition of the obtained sample at this stage of MD. These analyses that were taken from different regions of the milled powder do not show any serious compositional gradient and the average composition is being very close to the starting nominal composition of $Zr_{67}Ni_{33}$, as listed in Table. I.

The possibility of a MISSD (Ref. 15) has been explored by subjecting the obtained amorphous powders to longer MD time. Although the XRD pattern of the sample that was milled for 576 ks (not presented here) indicates that the obtained powder maintains its unique random structure, as far as indicated by broad primary and secondary diffraction maxima, the HRTEM image of this sample [Fig. 4(a)] shows obvious nanofringes of local ordered regions with different contrasts (see, for example, the indicated arrows) which are embedded in the amorphous matrix. Furthermore, the nano-

TABLE I. The local compositional analyses of ball-milled Zr_2Ni powders after 540 ks [see Fig. 3(a)] and 576 ks [see Fig. 4(a)] of mechanical disordering times. The analyses have been done using HRTEM and EDS techniques with an electron beam of 5 nm in diameter. The results are given in at. %.

	Zr	Ni
As-mechanically disordered for 540 ks		
I	67.1	32.9
II	66.8	33.2
III	66.5	33.5
IV	67.1	32.9
V	66.9	33.1
VI	67.0	33.0
VII	66.7	33.3
VIII	67.2	32.8
Average	66.9	33.1
As-mechanically disordered for 576 ks		
I	66.6	33.4
II	66.9	33.1
Average	66.8	33.2

beam diffraction pattern (NBDP) that was taken from region I in Fig. 4(a) shows a halo-diffraction pattern coexisted with several spots [Fig. 4(b)], implying the precipitation of a crystalline phase in the residual amorphous matrix. The EDS analytical results (Table I) of regions I and II could not detect any sharp compositional fluctuations between the selected neighbor regions (I and II), implying the homogeneity of the obtained product at this stage of MD.

The formed metastable big-cube phase of this stage of milling consists of spherical nanocrystalline grains ranging from 20 to 75 nm in diameter, as presented in the dark field image (DFI) of Fig. 5(a). The appearance of sharp-ring fash-

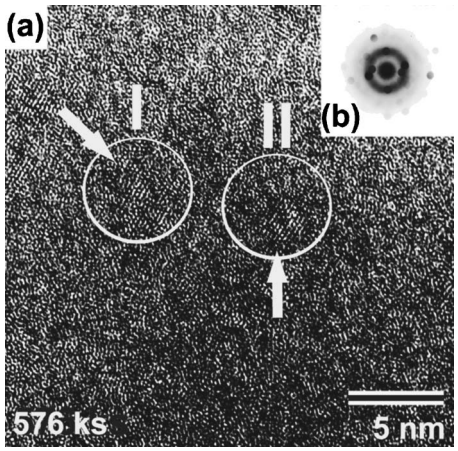

FIG. 4. (a) HRTEM image and (b) the corresponding NBDP of ball-milled Zr_2Ni powders after 576 ks of MD time. The indexed circles in image (a) refer to the EDS examined regions and the analytical results are listed in Table I. The fringes, which are embedded in the glassy matrix in image (a), belong to the big-cube Zr_2Ni metastable phase.

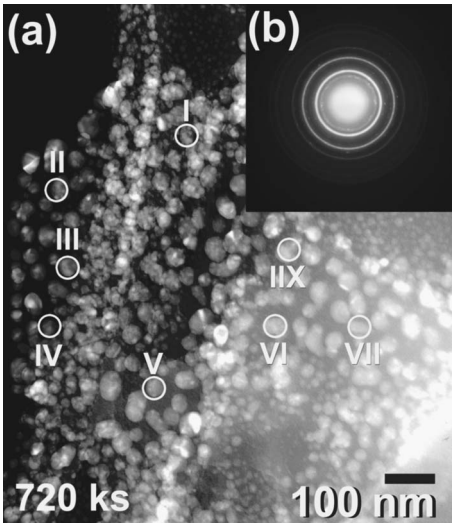

FIG. 5. (a) DFI and (b) the corresponding SADP of ball-milled Zr_2Ni powders after 720 ks of MD time. The indexed circles in image (a) refer to the EDS examined regions and the analytical results are listed in Table II.

ion at the corresponding SADP [Fig. 5(b)] with the absence of spotlike patterns suggests the formation of fine-grain structure and the disappearance of the previously formed amorphous phase. It is worth noting that the local EDS analyses that was taken from several regions in Fig. 5(a) do not show any surprising compositional differences (see Table II), indicating that the MISSD takes place in a typical polymorphous reaction.

More precise information about the local structure and composition of the powder of the end-product (900 ks) powders could be obtained by TEM and EDS analyses. The bright field image (BFI) of the powders at this stage of milling indicates the formation of nanomaterials that do not show any dramatic changes in composition (Table II) and have uniform nanostructure with spherical grains of less than 10 nm in diameter [Fig. 6(a)]. In addition, the indexed NBDP of a selected region indicates the presence of a single fcc phase in the milled powders with the absence of any other metastable phases (amorphous and/or big-cube phases).

TABLE II. The local compositional analyses of ball-milled Zr_2Ni powders after 720 ks [see Fig. 5(a)] and 900 ks [see Fig. 6(a)] of mechanical disordering times. The analyses have been done using HRTEM and EDS techniques with an electron beam of 5 nm in diameter. The results are given in at. %.

	Zr	Ni
As-mechanically disordered for 720 ks		
I	66.6	33.4
II	66.9	33.1
III	66.8	33.2
IV	67.0	33.0
V	66.7	33.3
VI	66.6	33.4
VII	66.9	33.1
VIII	67.1	32.9
Average	66.8	33.2
As-mechanically disordered for 900 ks		
I	67.1	32.9
II	67.0	33.0
III	66.9	33.1
IV	66.7	33.2
V	67.1	32.9
VI	66.8	33.2
VII	66.7	33.3
Average	69.9	33.1

From the above structural and compositional analyses, we can conclude that the mechanical disordering of tetragonal-Zr_2Ni powder takes place in the following fashion:

$$\text{Tetragonal } Zr_2Ni \text{ phase} \xrightarrow{\text{MD for 173 ks}} \text{Metastable fee-}Zr_2Ni \text{ phase} \xrightarrow{\text{MD for 360 ks}} \text{Metastable big-cube } Zr_2Ni \text{ phase} \xrightarrow{\text{MD for 540 ks}}$$

$$\text{Metastable amorphous } Zr_2Ni \text{ phase} \xrightarrow{\text{MD for 720 ks}} \text{Metastable big-cube } Zr_2Ni \text{ phase} \xrightarrow{\text{MD for 806 ks}} \text{Metastable fee-}Zr_2Ni \text{ phase}.$$

B. Thermal stabilities

The thermal stabilities of the three metastable products (glassy, big-cube, and fcc-Zr_2Ni alloys) that are yielded cyclically during the ball-milling process were examined by DSC. The DSC thermograms of these products are displayed in Figs. 7–9 after selected MD times. The DSC scan of the sample that was obtained after 173 ks of MD time reveals a single exothermic peak at 941 K [Fig. 7(a)]. The x-ray analysis of the sample taken after this DSC run shows the forma-

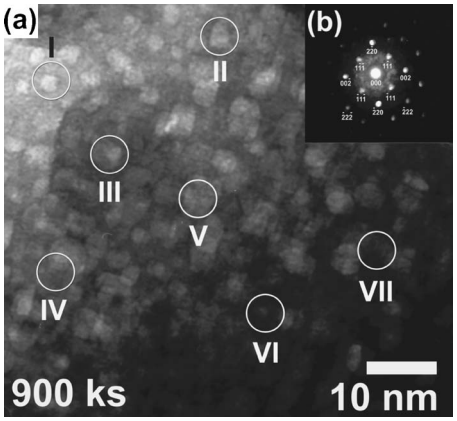

FIG. 6. (a) BFI and (b) the corresponding SADP of ball-milled Zr_2Ni powders after 720 ks of MD time. The indexed circles in image (a) refer to the EDS examined regions and the analytical results are listed in Table II.

tion of tetragonal-Zr_2Ni phase. The enthalpy change of crystallization $\Delta H_x^{fcc\rightarrow ordered}$ is calculated from the area under the exothermic peak in Fig. 7(a) and found to be −2.28 kJ/mol. $\Delta H_x^{fcc\rightarrow ordered}$ here is considered as the heat of formation of tetragonal-Zr_2Ni alloy.

However, this exothermic reaction still appears in the DSC curve of the sample that was milled for 360 ks of MD time [Fig. 7(b)]; the general feature of the thermograms is changed, characterized by the appearance of a low-temperature broad exothermic reaction that took place at 806 K. The XRD pattern of the sample that taken after the first exothermic reaction (850 K) shows the formation of metastable fcc-Zr_2Ni phase. The enthalpy change of crystallization $\Delta H_x^{big\ cube\rightarrow fcc}$ that realized due to this exothermic reaction is calculated and found to be −0.86 kJ/mol. Here, the $\Delta H_x^{big\ cube\rightarrow fcc}$ is considered as the heat of formation of metastable fcc-Zr_2Ni alloy. In this DSC scan [Fig. 7(b)], the area under the second exothermic reaction, which is considered as $\Delta H_x^{fcc\rightarrow ordered}$, is calculated to be −2.13 kJ/mol. Thus, the total enthalpy change of crystallization $\Delta H_x^{big\ cube\rightarrow fcc\rightarrow ordered}$ ($\Delta H_x^{big\ cube\rightarrow fcc\rightarrow ordered} = \Delta H_x^{big\ cube\rightarrow fcc} + \Delta H_x^{fcc\rightarrow ordered}$) is −2.99 kJ/mol.

Both peaks tend to disappear and becoming hardly visible when the MD time increases to 432 ks [Fig. 7(c)], whereas new peaks appear at this DSC scan. However, the first reaction, which is an endothermic type and refers to the glass transition temperature (T_g) of the formed glassy powders, can be seen hardly at 691 K; the second peak, which is an exothermic reaction and results due to the crystallization (T_x) of the glassy phase, is obvious and takes place at 736 K (onset temperature), as shown in Fig. 7(c). These two opposite reactions became more pronounced for those samples that were obtained after 470 ks [Fig. 7(d)] and 540 ks [Fig. 8(a)] of MD time. This implies an increase in the volume fraction of the formed glassy phase. The x-ray analysis of the sample that was obtained after completing this DSC run (750 K) shows the formation of tertragonal-Zr_2Ni phase, suggesting a glassy-ordered phase transformation at the observed T_x. It is worth noting that the onset temperature of both reactions does not change markedly, suggesting the absence of any compositional changes during the MD procedure. The wide value of the supercooled liquid region ΔT_x (ΔT_x, equal to $T_x - T_g$ at 46 K) for a binary metallic system suggests that the ball-milled Zr_2Ni alloy has a good glass-forming ability. Moreover, the enthalpy change of crystallization $\Delta H_x^{glassy\rightarrow ordered}$ of the glassy phase that is calculated from the area under the exothermic reaction in Fig. 8(a) is found to be −9.2 kJ/mol.

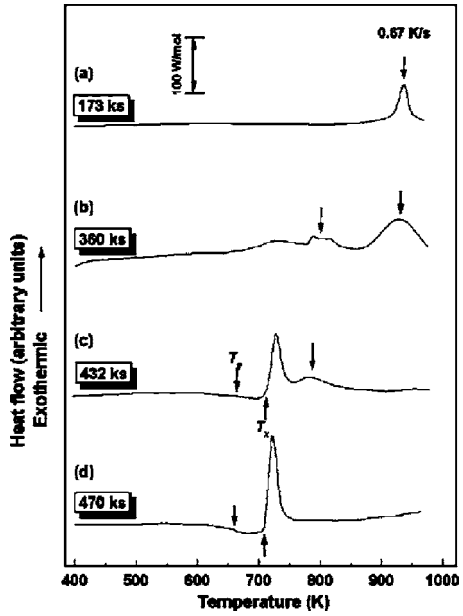

FIG. 7. DSC thermograms of ball-milled Zr_2Ni powders after (a) 173 ks, (b) 360 ks, (c) 432 ks, and (d) 470 ks of MD time.

The DSC scan for the sample that was obtained after 576 ks of MD time [Fig. 8(a)] shows a different feature with respect to the intensity of the exothermic reaction that is

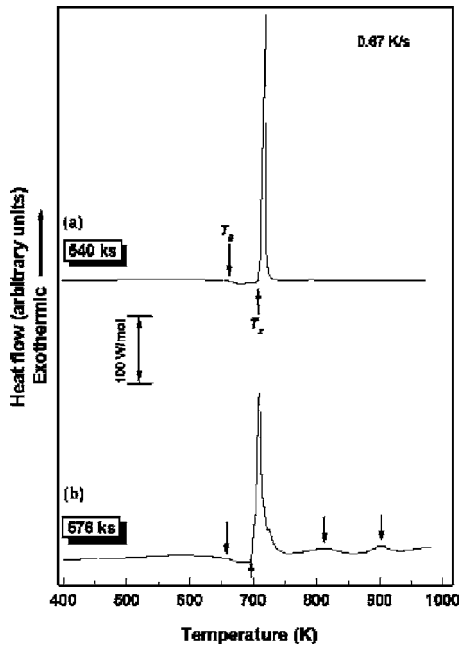

FIG. 8. DSC thermograms of ball-milled Zr_2Ni powders after (a) 540 ks and (c) 576 ks of MD time.

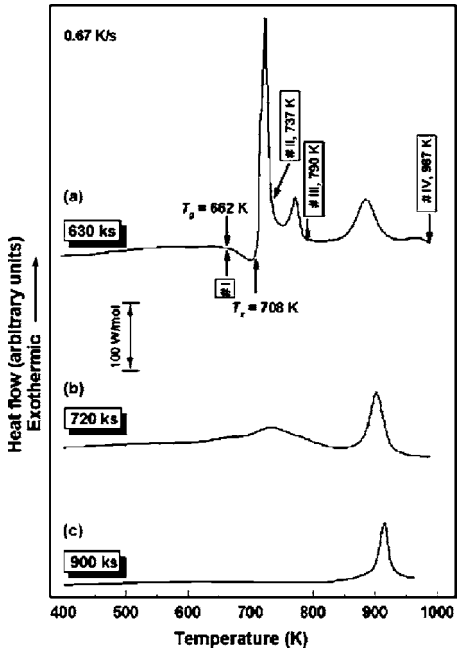

FIG. 9. DSC thermograms of ball-milled Zr_2Ni powders after (a) 630 ks, (b) 720 ks, and (c) 900 ks of MD time. The XRD patterns of the annealed samples at I, II, III, and IV are shown in Fig. 10 [(a), (b), (c), and (d), respectively].

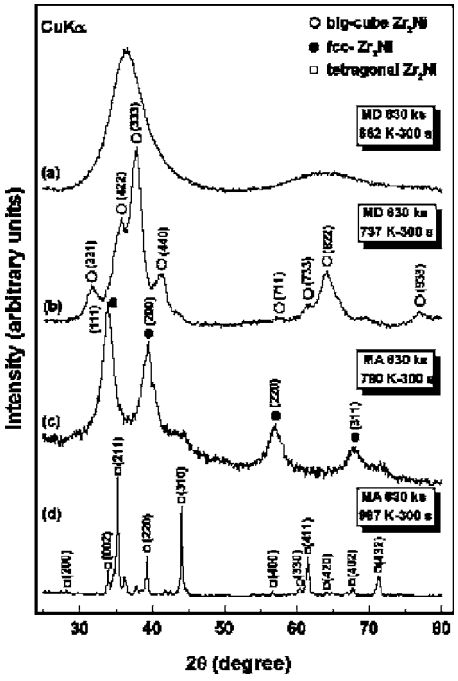

FIG. 10. The XRD patterns of ball-milled Zr_2Ni powders after ball milling for 630 ks of MD time plus annealing at (a) 662 K, (b) 737 K, (c) 790 K, and (d) 987 K. The annealing procedure was performed in a DSC under purified (99.9995 wt. %) Ar gas flow for 180 s.

becoming weak. In addition, the crystallization process takes place throughout several stages, indicated by a series of exothermic reactions, which are grown and becoming more visible for the sample that milled for 630 ks of MD time [Fig. 9(a)]. All of these events suggest a drastic decreasing of the formed glassy phase and a grown of new phase(s). It is worth mentioning that the thermal characterization of the residual glassy phase, characterized by T_g, T_x, and ΔT_x does not change, implying the absence of any compositional changes.

Contrary to the first exothermic reaction that appeared in the scan of Fig. 9(a), the second exothermic peak is taking place widely at 756 K. The last reaction of this DSC scan, however, takes place at higher temperature, as high as 850 K.

In order to explore the origin of the above-mentioned reactions, four individual heating runs were achieved for the sample, which was milled for 540 ks of MD time and each sample was checked carefully by x-ray analysis. These samples [I, II, III, and IV, Fig. 9(a)] were individually postannealed at temperatures of 662, 737, 790, and 987 K, respectively, for 300 s in the DSC under flow of pure argon.

The sample (I), which was annealed at 662 K, maintains its original characterizations of having a random structure without any devitrifications to any metastable phase(s), suggested by the clear broad diffused halos that are visible in Fig. 10(a). Annealing of this glassy phase at 737 K [II in Fig. 9(a)] (after its crystallization peak) leads to a devitrification into a metastable big-cube phase [Fig. 10(b)], similar to that one obtained after 360 and 720 ks of MD times [see Figs. 1(c) and 2(a), respectively].

This formed metastable big-cube Zr_2Ni phase does not maintain its unique crystalline structure and transformed into another metastable phase of fcc-Zr_2Ni upon postannealing the powders at 790 K [III in Fig. 9(a)], as was confirmed by the XRD pattern in Fig. 10(c). It is worth noting that this formed metastable fcc phase has almost the same a_0 of those products which yielded after 173 and 806 ks of MD times [Figs. 1(b) and 2(b) respectively]. The XRD pattern of the sample powder [IV in Fig. 9(a)], which was annealed after achieving the last exothermic peak (987 K), indicates that this exothermic reaction takes place due to transformation of the metastable fcc-Zr_2Ni into a the most-stable phase of tetragonal-Zr_2Ni [Fig. 10(d)], in good agreement with that XRD pattern of the starting (before milling) powders of Zr_2Ni [Fig. 1(a)].

The area under the first exothermic reaction in Fig. 9(a) presents the heat formation of big-cube Zr_2Ni phase upon annealing the Zr_2Ni glassy phase that is obtained after 630 ks of MD time ($\Delta H_x^{glassy\rightarrow big\ cube}$ or $\Delta H_{big\ cube}^{for}$), and found to be −5.89 kJ/mol. The $\Delta H_x^{big\ cube\rightarrow fcc}$ or the heat formation of metastable fcc-Zr_2Ni alloy [ΔH_{fcc}^{for}, the calculated area under the second exothermic peak in Fig. 9(a)] is found to be −0.93 kJ/mol. The $\Delta H_x^{fcc\rightarrow ordered}$ [the area under that last exothermic peak in Fig. 9(b)] or the so-called heat formation of ordered-Zr_2Ni alloy ($\Delta H_{ordered}^{for}$) is calculated and found to be −1.74 kJ/mol.

Thus, the total heat formation of tetragonal Zr_2Ni alloy can be calculated as $\Delta H_{ordered}^{for}$ ($\Delta H_x^{glassy\rightarrow big\ cube\rightarrow fcc\rightarrow ordered}$) $=\Delta H_x^{glassy\rightarrow big\ cube}+\Delta H_x^{big\ cube\rightarrow fcc}+\Delta H_x^{fcc\rightarrow ordered}$. Here, $\Delta H_{ordered}^{for}$, which is calculated to be −8.65 kJ/mol, has a very close value to the $\Delta H_{ordered}^{for}$ (−9.2 kJ/mol) which obtained upon single phase transformation of glassy-ordered phase transformation for the sample that was milled for 540 ks of MD time.

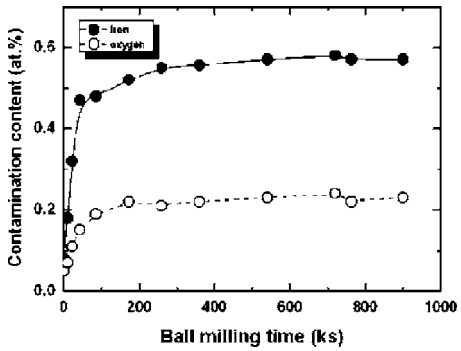

FIG. 11. Effect of mechanical disordering time, MD time on iron, and oxygen contamination contents in the ball-milled Zr_2Ni powders.

The DSC scan of the powders, which were milled for 720 ks (originally metastable big-cube phase) is displayed in Fig. 9(b). One can notify the disappearance of the endothermic reaction, which indicates the absence of the glassy phase [Fig. 9(b)]. The disappearance of the glassy phase is also indicated by the absence of the sharp exothermic reaction, which was replaced by a broad exothermic peak that took place at 731 K [Fig. 9(b)]. At a temperature well above this broad exothermic peak (832 K), this big-cube Zr_2Ni phase transformed into a more stable phase of fcc-Zr_2Ni, as examined by the x-ray analysis.

Finally, we have examined the thermal stability of the metastable fcc-Zr_2Ni powders that were obtained after 900 ks of MD time. The DSC curve of this alloy is shown in Fig. 9(c). Whereas the second exothermic peak in Fig. 9(b) was vanished, the high-temperature exothermic reaction still appears at a peak temperature of 900 K. The XRD pattern of the sample, which was taken after annealing the powders at 985 K for 300 s (not shown here), implies that this exothermic reaction takes place by the transformation of the metastable fcc-Zr_2Ni into the most-stable phases of tetragonal-Zr_2Ni. We can then conclude that the phase transformations that took place upon postannealing the obtained glassy powders after 540 ks of MD can be summarized as follows:

$$\text{Glassy } Zr_2Ni \text{ phase} \xrightarrow{737\ \text{K},300\ \text{s}} \text{Metastable big-cube } Zr_2Ni \text{ phase} \xrightarrow{790\ \text{K},300\ \text{s}} \text{Metastable fcc-}Zr_2Ni \text{ phase} \rightarrow \text{tetragonal } Zr_2Ni \text{ phase}.$$

Milled samples were chemically analyzed and plotted in Fig. 11 as a function of MD times. The iron, which comes from the stainless-steel milling tools, monotonically increased with increasing MD time and saturated at a level of 0.57 at. % after 540 ks of MD time. Likewise, the oxygen contamination increases significantly during the first kiloseconds of milling to a value of 0.19 at. % after 86 ks of the MA time. At the final stage of milling (173–900 ks), the oxygen content saturates at a value of 0.24 at. %.

IV. DISCUSSION

High-energy ball-milling technique, starting from intermetallic tetragonal-Zr_2Ni powders leads to the formation of three different kinds of Zr_2Ni metastable phases yielded with changing the milling times. This cyclic-phase transformations in the metastable amorphous and glassy alloys was first reported in 1997 by El-Eskandarany *et al.*[26] In year 2000 and based on this new finding, Sluiter and Kawazoe[27] introduced a simple model for such cyclic phenomenon, specially when El-Eskandarany *et al.* have reported that such phenomenon can occur in different families of amorphous alloys.[28,29] Since then, different materials science scientists who are interested in amorphous and metallic glassy alloys studied the cyclic phenomenon in various metallic metastable alloys (e.g., Refs. 11 and 30–32).

A. Ordered-disordered phase transformations

The formation of metastable phases by ball milling the powders of intermetallic Zr_2Ni (the most stable state) requires raising in the free energy of the ordered phase. During the early stage of MD (0–173 ks), tetragonal-Zr_2Ni alloy powders, which absorb significant amounts of energy, tend to transform into a new metastable phase of fcc-Zr_2Ni with a_0 of 0.451 nm.[33] This metastable phase usually appears as a final or an intermediate product during mechanical alloying of some Zr-based alloys.[14,15] Moreover, it has been shown[34] that ball milling of pure hcp-Zr metal leads to the formations of elemental fcc-Zr metal with a_0 of 0.46 nm. The plastic strain that is yielded as a result of the ball collisions leads to a lattice expansion of the obtained fcc-Zr_2Ni metastable phase. This structural instability is translated to a raise in the ΔG from a more stable phase to a less stable phase. After 360 ks of MD time [Fig. 1(c)], the obtained nonequilibrium fcc-phase transformed to another metastable phase of big-cube Zr_2Ni alloy [$E9_3$ structure, space group $Fd3m$ (Ref. 24)] with a_0 of 1.226 nm. Likewise, the fcc-metastable phase, with increasing milling time (540 ks), affects the stability of the obtained big-cube phase, resulting to an increase in the ΔG from point and the formation of a less stable phase of glassy Zr_2Ni alloy powders after 540 ks milling time [Figs. 1(d) and 3].

The HRTEM and EDS observations strongly indicate that the glassy Zr_2Ni powders tends to crystallize into a meta-

stable big-cube phase of the same composition upon further ball-milling time to 576–630 ks (see Figs. 4 and 9(a) and Table I). This associates a drastic change in the crystallization behavior where the crystallization takes place through three individual steps [Figs. 8(b) and 9(a)]. The existence of such primary nanophase in the glassy matrix increases with increasing ball milling times and the remained mole fraction of the glassy phase transformed into a big-cube Zr_2Ni upon milling for 720 ks [Figs. 2(a) and 5].

The results have also shown that the obtained big-cube phase tends to transform into an fcc-Zr_2Ni metastable phase upon further milling (806–900 ks), as shown in Figs. 2(b), 2(c), and 6. Based on the fact that all of the formed metastable phases via ball-milling technique (glassy, big cube, and fcc) (1) transform to the most stable phase of a tetragonal-Zr_2Ni phases upon heating during the DSC measurements and (2) are nearly similar in compositions (Tables I and II); all of these strongly suggest that the phase transformation that took place via MISSD is a polymorphous type where the crystallization takes place without any compositional changes.

Our results cannot be explained by the concept of temperature rise during milling because the obtained metastable phases are periodically transformed to each other (upon further milling time and under the same milling conditions. This implies that the local temperature should be the same while the phase transformations took place. In this context, the recorded vial temperature during the ball-milling process is far below (~372 K) than the required temperatures for appropriate structural change in the milled powder. In addition, the recorded temperatures of the vials during the different stages of milling remained constant even as the transformations take place.

The presence of significant heterogeneity in the ball-milled powders is a severe problem and realized here to be responsible of such cyclic phase transformations. The EDS analyses of elemental Zr and Ni in the ball-milled powders that were obtained after different milling times (Tables I and II) have not shown any significant concentration gradients or compositional fluctuation, indicating that the glassy and metastable phases (big cube and fcc) are similar in composition and are homogeneous on the atomic scale.

Another possible factor that could lead to such periodic transformations is the introduction of contamination in the ball-milled powders. The compositional analyses (chemical and EDS analyses) have shown that the powders of the final product (900 ks) were contaminated with low levels of iron and oxygen (Fig. 11). Aside from such a low level of impurities, they remain constant, whereas the transformations take place.

Since ball milling introduces great number of vacancies, lattice defects, grain boundaries, and surfaces, the ball-milled powders store significant amounts of energy.[11] In the initial milling stage, crystalline powders are mechanically crushed and this enhances the atomic disordering. The defects and interface area can increase the enthalpy for pure metallic ball-milled powder by about 7.4 kJ/mol (Ref. 34) and perhaps more for glassy alloys, where destruction of the short-range order can contribute an additional enthalpy. It has been suggested that the order enthalpy in transition metal alloys can be as large as 10 kJ/mol.[35,36] When the long-range periodic structure is destroyed by introduction of defects, a glass phase is obtained as a metastable state. In the milling process, friction between balls and balls and the lining surface of a vial also generates frictional heat. Such heat does not accelerate the atomic imperfections. We believe that the mechanical deformation during ball milling induces the periodic phase transformations without significant aid of local temperature, typical to the room-temperature deformation that was previously observed in several amorphous alloys.

V. CONCLUSIONS

Our results demonstrated cyclic metastable phase transformations during mechanical disordering of tetragonal-Zr_2Ni intermetallic powders using high-energy ball mill. After 173 ks of milling time, an fcc-Zr_2Ni metastable phase is obtained and transformed into ordered-Zr_2Ni upon heating to 941 K. The enthalpy change of transformation $\Delta H^{fcc\rightarrow ordered}$ was found to be −2.28 kJ/mol. This fcc phase transforms into another metastable phase (big-cube Zr_2Ni) upon milling to 360 ks using the same milling conditions. This big-cube Zr_2Ni transforms to fcc-Zr_2Ni at 850 K with $\Delta H^{big\text{-}cube\rightarrow fcc}$ of −0.86 kJ/mol. A single glassy phase of Zr_2Ni is obtained as a result of further milling for 540 ks. This glassy phase that has T_g, T_x, and ΔT_x of 691, 736, and 41 K, respectively, transforms into ordered-Zr_2Ni with $\Delta H_x^{glassy\rightarrow ordered}$ of −9.2 kJ/mol. Increasing the ball-milling time (720 ks) leads to devitrification of the obtained glassy phase and the formation of nanocrystalline big-cube Zr_2Ni powders. This big-cube phase is no longer in the milled powders, when the milling time increased to 806 ks, and transformed into the same metastable phase of fcc-Zr_2Ni that was early obtained after 173 ks of the time. We have attributed these transformations, which took place in the ball mill to the disability of the formed metastable phases to withstand against the impact and shear forces that are generated by the milling media (balls). When the milling time is increased, the formed metastable phase is subjected to crystalline defects (points and lattice defects) that rise or lowers the free energy of the formed phases, being dependant on the milling time. Our results cannot be explained by the concept of the local temperature rise during milling because the obtained metastable phases are periodically transformed to each other upon further milling time and under the same milling conditions.

*Author to whom correspondence should be addressed. Present address: Technology Development and Scientific Services Sector, Academy of Scientific Research and Technology, Ministry of Scientific Research, 101 Kasr Al-Aini Street, Cairo 11516, Egypt. FAX: +202-7953785. Electronic address: msherif@www.eleskandarany.com

[1] K. Klement, R. H. Willens, and P. Duwez, Nature (London) **187**, 869 (1960).
[2] A. L. Greer, Science **267**, 1947 (1995).
[3] A. J. Drehman, A. L. Greer, and D. Turnbull, Appl. Phys. Lett. **41**, 716 (1982).
[4] A. Inoue, W. Zhang, T. Zhang, and K. Kurosaka, Mater. Trans., JIM **42**, 1149 (2001).
[5] A. Inoue, in *Bulk Amorphous Alloys: Practical Characteristics and Applications*, 1st ed., edited by M. Magini and F. H. Wöhlbier (Trans Tech, Switzerland, 1999), pp. 140–141.
[6] R. J. Gottschall, Mater. Trans., JIM **42**, 548 (2001).
[7] A. Inoue, in *Bulk Amorphous Alloys: Practical Characteristics and Applications*, 1st ed., edited by M. Magini and F. H. Wöhlbier (Trans Tech, Switzerland, 1999), p. 140.
[8] A. Peker and W. L. Johnson, Appl. Phys. Lett. **63**, 2342 (1993).
[9] C. C. Koch, O. B. Cavin, C. G. MacKamey, and J. O. Scarbourgh, Appl. Phys. Lett. **43**, 1017 (1983).
[10] M. Sherif El-Eskandarany, *Mechanical Alloying for Fabrication of Advanced Engineering Materials*, 1st ed. (William Andrew, New York, 2001), p. 142.
[11] M. Sherif El-Eskandarany and Inoue, Metall. Mater. Trans. A **33**, 2145 (2002).
[12] M. Sherif El-Eskandarany, J. Saida, and A. Inoue, Acta Mater. **50**, 2725 (2002).
[13] M. Sherif El-Eskandarany, J. Saida, and A. Inoue, J. Mater. Res. **18**, 250 (2003).
[14] M. Sherif El-Eskandarany, J. Saida, and A. Inoue, Acta Mater. **51**, 1481 (2003).
[15] M. Sherif El-Eskandarany, J. Saida, and A. Inoue, Acta Mater. **51**, 4519 (2003).
[16] M. Sherif El-Eskandarany and A. Inoue, Mater. Trans., JIM **43**, 770 (2002).
[17] M. Sherif El-Eskandarany, W. Zhang, and A. Inoue, J. Alloys Compd. **350**, 222 (2003).
[18] M. Sherif El-Eskandarany, S. Ishihara, and A. Inoue, J. Mater. Res. **18**, 2435 (2003).
[19] M. Sherif El-Eskandarany, Satoru Ishihara, Wei Zhang, and A. Inoue, Metall. Mater. Trans. A **36**, 141 (2005).
[20] H. Y. Bai, C. Michaelsen, C. Gente, and R. Bormann, Phys. Rev. B **63**, 064202 (2001).
[21] M. Sherif El-Eskandarany, M. Omori, and A. Inoue, J. Mater. Res. **20**, 2845 (2005).
[22] M. Sherif El-Eskandarany and A. Inoue, J. Mater. Res. **21**, 976 (2006).
[23] M. Sherif El-Eskandarany and A. Inoue, Metall. Mater. Trans. A **37**, 2231 (2006).
[24] M. Sherif El-Eskandarany, K. Aoki, and K. Suzuki, J. Alloys Compd. **177**, 229 (1991).
[25] Z. Altounian, E. Batalla, J. O. Strom-Olsen, and J. L. J. Walter, Appl. Phys. Lett. **61**, 149 (1987).
[26] M. Sherif El-Eskandarany, K. Aoki, K. Sumiyama, and K. Suzuki, Appl. Phys. Lett. **70**, 1679 (1997).
[27] M. Sluiter and Y. Kawazoe, Acta Mater. **47**, 475 (2000).
[28] M. Sherif El-Eskandarany, K. Aoki, K. Sumiyama, and K. Suzuki, Scr. Mater. **36**, 100 (1997).
[29] M. Sherif El-Eskandarany, K. Aoki, K. Sumiyama, and K. Suzuki, Metall. Mater. Trans. A **30**, 1877 (1999).
[30] M. Sherif El-Eskandarany, K. Aoki, K. Sumiyama, and K. Suzuki, Acta Mater. **50**, 1113 (2002).
[31] T. H. Courtney and J. K. Lfe, Philos. Mag. **85**, 153 (2005).
[32] William C. Johnson, Jong K. Lee, and G. J. Shiflet, Acta Mater. **54**, 5123 (2006).
[33] I. Mann, P. P. Chattopadhyay, F. Banhart, and H.-J. Fecht, Appl. Phys. Lett. **81**, 4136 (2002).
[34] H. J. Fecht, E. Hellstein, Z. Fu, and W. L. Johnson, Metall. Trans. A **21**, 2333 (1990).
[35] S. R. Harris, D. H. Pearson, C. M. Garland, and B. Fults, J. Mater. Res. **6**, 1 (1991).
[36] M. Sluiter and P. E. A. Turchi, Phys. Rev. B **46**, 2565 (1992).